The use of light scattering and ion chamber responses for the detection of fires in diesel contaminated atmospheres

Charles D. Litton*

National Institute for Occupational Safety and Health, Pittsburgh Research Center, Cochrans Mill Road, Pittsburgh, PA 15236, USA

Received 20 February 2001; received in revised form 4 June 2001; accepted 27 August 2001

Abstract

Experiments were conducted to determine the optical scattering properties of diesel particulate matter (DPM) and various combustion aerosols from both flaming and smoldering combustion sources at discrete angles of 15° and 30° in the forward direction and at a light source wavelength of 635 nm using a simple light scattering module. In addition to the scattering data, simultaneous measurements were made of the total aerosol mass concentration; light extinction at an average wavelength of 546 nm; and the response of a common bipolar ion chamber typical of residential smoke detectors modified to allow the aerosols to flow through the chamber. The results of these experiments indicate, for DPM and combustion aerosols, the intensities per unit mass concentration depend not only upon whether the aerosol is DPM or combustion aerosol but also upon the type of combustion aerosol. The results also indicate that the ion chamber responses are greatest for DPM, followed by the response to flaming combustion aerosols (FCA) and lowest for smoldering combustion aerosols (SCA). For light scattering, the greatest intensities are found for SCA, followed by the intensities from FCA, and lowest for DPM. This report describes the experiments, their results, and the use of these results to develop design criteria for early warning fire sensors capable of the rapid and reliable detection of fires in atmospheres that may or may not be contaminated by the products produced from diesel engines.

*Tel.: +1-412-386-6752; fax: +1-412-386-6561.
E-mail address: chl3@cdc.gov (C.D. Litton).

0379-7112/02/$ - see front matter
PII: S0379-7112(01)00059-5

1. Introduction

1.1. Background

Fire sensors that detect the smoke and gases produced during the early stages of developing fires are often compromised by the presence of background levels of aerosols or gases that mimic the signatures of the developing fires, often resulting in frequent false, or nuisance, sensor alarms. When this frequency is high, the tendency is to either ignore sensor alarms, or to de-energize the sensors, with the potentially catastrophic consequence that an actual fire is not detected. For instance, previous surveys of installed residential smoke detectors [1], indicated that nearly 20% of the detectors did not have functioning power sources, and of these, about one-third were intentionally disconnected because of nuisance alarms. In another study [2], 273 smoke detectors were examined by fire departments subsequent to the extinguishment of residential fires that went undetected. Of these, 159 (59%) were found to be disconnected from the power source.

Nuisance alarms can occur in industrial settings, as well, with similar actions and consequences, real alarms that may be ignored or sensors that are disconnected from their power source, resulting in fires that destroy both life and property. A recent workshop [3] highlighted the problems associated with nuisance alarms in aircraft cargo areas and critical telecommunications systems and stressed the need to develop improved fire sensing systems and test procedures for installed fire detection systems. Fire detection in underground mines and tunnels is often compromised by exhaust products from diesel engines or other vehicles, or by routine procedures, such as welding or cutting. In mines, and to a somewhat lesser degree in tunnels, dust is an ever-present problem.

A significant level of research is being done to resolve some of these problems. For smoke, efforts continue to more accurately and completely define the properties of smoke produced from different sources [4–6] and to develop improved techniques for smoke measurement [7]. Characterizing the signatures of interfering sources using multi-sensor arrays coupled with neural networks or other multi-signature alarm algorithms [8–10] offer significant promise in many applications. But the use of these multi-sensor approaches are generally application-specific in that different applications may require different sensors and the necessary algorithms can vary significantly from one application to the next. In some of these approaches, it is not only the relative signals from different sensors, but also the manner in which these signals vary with time, that allow for the discrimination, but incorporating time into the process can also be detrimental to the early warning capability of the system. In underground mines, multi-sensor approaches and simpler gas ratio techniques [11,12] have also been used with varying degrees of success. In the mine application, and others, the use of multi-sensor packages and software to process the signals and make decisions increases not only the complexity, but also the cost of the system, not only in terms of base, initial expense, but also in terms of system maintenance and sensor replacement.

One alternative to these approaches is the development of simple, stand-alone fire sensors that capitalize on the differences between common, interfering aerosol and/or gas backgrounds and those that result from developing fires so that the discrimination occurs via the sensor and its associated electronics rather than from a potentially more complex processing algorithm. This paper describes such a sensor as it applies to the detection of fires in underground mines, where a major background source is due to the emissions from diesel engines that are used routinely in day-to-day mining operations.

1.2. Overview

In the initial stages of this research, the objective was to study, both theoretically and experimentally, the angular distribution of scattered light from a polydisperse system of particles produced from diesel engines (diesel particulate matter—DPM) and from both flaming and smoldering combustion as part of an effort to develop fire sensors that can reliably detect a developing fire in atmospheres contaminated by the exhaust products from diesel engines, since these products represent signatures similar to those from fires and can cause conventional products of combustion fire sensors to produce frequent false, or nuisance, alarms that degrade the early warning capability and reliability of the fire sensor. Previous research in this area [13] had partially quantified the angular scattering signatures of DPM and various combustion aerosols, with the result that DPM and combustion aerosols do, indeed, produce different characteristic light scattering signatures, yet additional research was necessary before final conclusions could be reached relative to the effectiveness and feasibility of this approach. This report addresses and assesses the potential of light scattering and, as it evolved, ion chamber response, and/or combinations of the two, as they apply to the detection of developing fires and to the discrimination between aerosols produced from fires and those produced from diesel engines.

1.3. Light scattering

The use of light scattering as a technique for detection of developing fires is not new. Light scattering is attractive primarily because it is simple, generally inexpensive to implement, and highly sensitive. Currently, there exist many detectors that are available commercially that utilize this technique, generally referred to as photo-electric type smoke detectors, although significant differences may exist among the various detectors, such as angle(s) for detection, light source wavelength, etc. For DPM and combustion aerosols, previous studies [13] had shown that the Mie theory is not adequate to describe their angular scattering properties, and that treatment of these particles as fractal-like aggregates is more appropriate, yielding much better agreement with the experimental angular scattering data. In addition, the angular intensities per unit mass, especially at forward angles less than about 30°, are greater by a factor of 2–3 for smoldering combustion aerosols (SCA) compared to flaming combustion aerosols (FCA). This difference in sensitivity results in a detector that is more sensitive to smoldering fires than to flaming fires, in direct

contrast to the sensitivity of ionization-type smoke detectors discussed below, where the highest sensitivity is expected for DPM and the lowest for SCA. The previous data also indicated that the angular intensities per unit mass are significantly lower for DPM than for aerosols from flaming combustion. These results are partially due to differences in size of the different aerosols and also to the volatile content of the different aerosols, where aerosols with a high volatile fraction, i.e., aerosols from smoldering combustion, tend to scatter light more efficiently.

1.4. Ion chambers

Ion chambers in the form of ionization-type smoke detectors have also been used routinely as early warning fire sensors since the mid 1970s. Typically, the source of ions in these types of ion chambers is a very low-level radioactive source of ^{241}Am. ^{241}Am decays via the emission of alpha particles (He atoms) and as these particles traverse the air space between two electrodes, both positive and negative ions are created. The positive ions drift to the negative electrode while the negative ions drift to the positive electrode. This separation of ions, coupled with the geometry of the chamber, creates a space charge that distorts the electric field and electric potential within the ion chamber. A third, floating electrode is generally located between the positive and negative electrode at a position where the electric potential reaches its maximum distortion, and the potential at this electrode is continuously measured. When aerosols enter the air space between the electrodes, the positive and negative ions rapidly attach to the aerosol particles, depleting the ion concentrations, which, in turn, reduces the distortion of the electric potential causing the potential at the floating electrode to increase.

Very early in the development of these chambers it was found that such detectors are more sensitive to aerosols produced from flaming combustion than they are to aerosols produced from smoldering combustion. The reason for this difference in sensitivity is the result of two factors. First, the response of an ionization chamber to the presence of an aerosol at low concentrations varies directly with the product of number mean particle diameter, d_G, and number concentration, n_O, or $d_G n_O$. Consequently, for aerosol sources that produce large number of very small particles, the sensitivity will be high. Second, when small particles form aggregates of much larger extent, high sensitivity will also result for low to moderate concentrations of these larger aggregates. Previous studies [13] indicate that the primary particle diameters for FCA and SCA are around 30 and 70 nm, respectively. FCA form aggregate particles containing 500–1000 of the primary particles, an average mass of around 1.5×10^{-14} g, and with an average radius of gyration, R_G, in the range of 350–400 nm. SCA tend to form aggregates containing roughly 100 primary particles, an average mass of around 2.5×10^{-14} g, and with an average R_G in the range of 200–250 nm. At an average mass concentration of 2×10^{-9} g/cm^3 (2 mg/m^3) the number of flaming aggregates per cm^3, n_O, is around 1.3×10^5 while the number of smoldering aggregates is about 8×10^4. If d_G is set equal to $2R_G$, then for flaming aggregates, $d_G n_O$ is in the range of 4.5–5, while for smoldering aggregates the value is in the range of 1.6–2.0. These simple calculations indicate that the ion chamber is 2–3

times more sensitive to FCA than to SCA. If it were assumed that no aggregation occurred, then the difference in sensitivities would be even greater.

Similarly, these research results indicated that the primary particle diameter for DPM is in the range of 25 nm and that these primary particles aggregate to form filaments of irregular shape with a typical radius of gyration, R_G, in the range of 450–500 nm. In addition, these aggregates are typically composed of about 1500 individual primary particles. If it is assumed that each primary particle has a density of 1.5 g/cm^3, then a simple calculation indicates that the mass of one aggregate particle containing 1500 primary particles is of the order of 2×10^{-14} g, and that the number of aggregates per cm^3 necessary to achieve a mass concentration of 2×10^{-9} g/cm^3 (2 mg/m^3) is 1×10^5. If the number mean particle diameter is taken to be twice the radius of gyration, then the product, $d_G n_O$, is in the range of 9–10. This simple calculation implies that the ion chamber is about 2–3 times more sensitive to DPM than to aerosols from flaming combustion and about 5–6 times more sensitive to DPM than to aerosols from smoldering combustion.

Regardless of the exact relative values, these numbers indicate that an ion chamber should be significantly more sensitive to DPM than to aerosols produced from either flaming or smoldering combustion while light scattering sensitivities are in the reverse order. These relative sensitivities would mean that if the ratio of ion chamber response to light scattering response were obtained for the different aerosols, then a high value would result for DPM, a lower value for FCA, and a much lower value for SCA, and that this ratio could possibly be used to provide for a high degree of discrimination between the different aerosol types. To test this hypothesis, the response of a typical ion chamber and the angular intensities were measured for DPM, FCA, SCA and mixtures of DPM/FCA and DPM/SCA. The experiments conducted and their results follow.

2. Experimental

Experiments were conducted in the configuration shown in Fig. 1 and described in more detail in Ref. [14], where aerosols from either flaming or smoldering combustion are generated in a cubical enclosure measuring 0.30 m along each edge and then diverted into a standard smoke box through a variable-orifice iris that controlled the rate of aerosol accumulation within the smoke box. For DPM, the exhaust from a diesel generator was flowed into the cubical chamber via a 10.2 cm i.d. flexible hose and then diverted into the smoke box. Within the smoke box, two small fans provided for continuous mixing of the aerosol. The optical density of the aerosol was measured over a 1.483 m optical path using an incandescent lamp and a standard photocell with a peak response at a wavelength of 546 nm and a spectral response matching the spectral response of the human eye. During the experiments, aerosol samples were continuously extracted from a metal tube inserted into the top of the smoke box and flowed to the various measuring devices. In this configuration, data were obtained for flaming No. 2 diesel fuel (a small pool flame), flaming coal, flaming wood, flaming paper, flaming styrene–butadiene rubber (SBR), smoldering

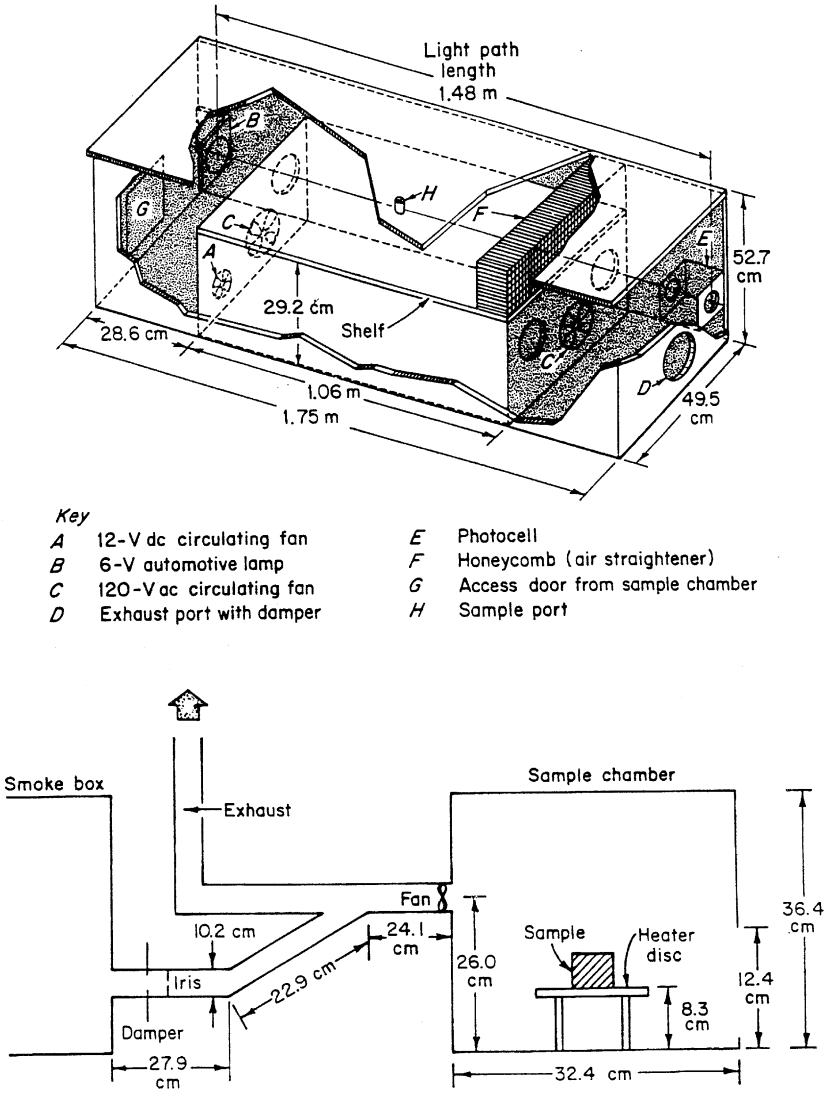

Fig. 1. Schematic of the smoke box and sample chamber in which the experiments were conducted.

coal, smoldering wood, smoldering SBR, and DPM from the exhaust of the diesel generator.

2.1. Measuring devices

During the experiments, a tapered element oscillating microbalance (TEOM) [15] was used to continuously measure the mass concentrations of aerosol. In the TEOM,

a small filter is mounted onto what amounts to a hollow tuning fork vibrating at a fixed frequency. Particles in the flow through this filter are deposited on the filter increasing the filter mass. As the filter mass increases, the frequency of vibration decreases proportionally.

For light scattering, several prototype scattering cells were fabricated and evaluated via some initial, exploratory experiments to arrive at the final scattering module, shown schematically in Fig. 2. The scattering module is a right circular disk with a diameter of 7.62 cm and a height of 2.54 cm. Two PIN-125DP/L photodiodes, with a square active detecting surface $1.27 \times 1.27\,\mathrm{mm}^2$, and with responsivities of 0.39 A/W at $\lambda = 635\,\mathrm{nm}$, were positioned, with their active surfaces located 3.2 cm from the disk center, to measure the angular intensities at 15° and 30°. The output signals from the two photodiodes were amplified and converted from current to voltage using a simple amplifier with a negative gain of 5×10^8. The air space between the photodiode and central scattering volume is cylindrical with a diameter of 0.20 cm. For this module, a small laser diode operating at a wavelength of 635 nm and an output power level of 5–6 mW, was used as the light source and the beam focused at the center of the scattering volume with a spot diameter of about 2 mm. In addition, for this module, the aerosols were flowed through the scattering volume at right angles to the direction of the laser diode beam.

For the scattering module, the actual scattering volumes vary inversely with the sine of the scattering angle, so that as the angle increases, the scattering volume decreases. Assuming the scattering volumes to be defined by the light source beam diameters d_{BEAM}, and the diameters of the cylindrical light paths from the beam to the detectors, d_{DET}, then the volumes at each angle may be calculated approximately from the expression

$$V(\theta) = (\pi/4) d_{\mathrm{DET}}^2 d_{\mathrm{BEAM}} / \sin(\theta). \tag{1}$$

For the dimensions defined above, the following approximate scattering volumes result: $V(15) = 0.02546\,\mathrm{cm}^3$ and $V(30) = 0.01318\,\mathrm{cm}^3$. The effect of a smaller scattering volume at 30° is to reduce the actual intensity by an additional factor of

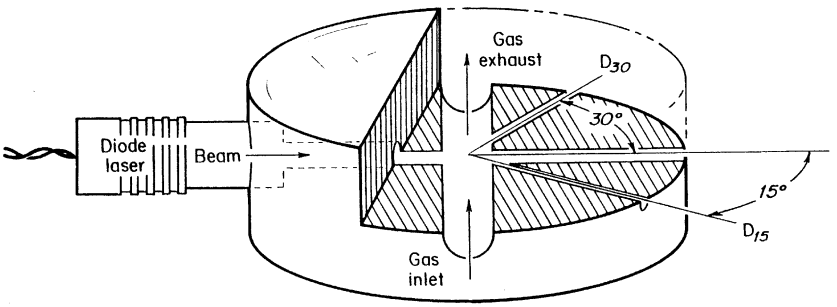

Fig. 2. Schematic of the light scattering module using a laser diode at $\lambda = 635\,\mathrm{nm}$ as the light source. In this chamber, aerosols are flowed through the scattering module normal to the direction of the diode laser beam.

1.93, assuming that the number of aerosol particles per unit volume are uniformly distributed.

The bipolar ion chamber used in these experiments, typical of ion chambers found in ionization-type smoke detectors, is shown schematically in Fig. 3. In this chamber, a 2.0 mm diameter source of ^{241}Am with an activity of 0.80 μCi and face coated with a 2.0 μm thick Pd foil, is placed in the center of the base of a small cylindrical cavity with a diameter of 0.95 cm and height of 0.45 cm. At the distance of 0.45 cm from the source surface, the chamber abruptly expands to form a larger cylinder with a diameter of 3.25 cm. At the top of this larger cylinder is the negative electrode with its surface located a total distance of 1.90 cm from the surface of the source, which also serves as the positive electrode. Within these two volumes, both positive and negative air ions are created so that the chamber is referred to as a bipolar chamber. At the top of the smaller cylinder (0.45 cm away from the source) is a floating conductor used to measure the electric potential at this plane in the chamber. The position of this floating conductor corresponds approximately to the plane of maximum distortion of the potential within the chamber. When operated at the standard voltage of 9.0 V, the potential at this plane is generally in the range of 3.4–3.9 V, a result of distortion of the electric field and potential due to space charge effects. If there were no source in the chamber, a simple electrostatic analysis indicates that the potential at this plane would be ~6.85 V. The difference, 2.95–3.45 V, represents the dynamic range for the potential at this position. When aerosols enter the chamber, they deplete the ions via attachment, and cause the potential to increase. Normally, aerosols enter the chamber via diffusion or via convective air flows, but for these experiments, the chamber was modified so that aerosols could be flowed through the chamber, entering and exiting at two opposite points halfway between the floating conductor and the top, negative electrode.

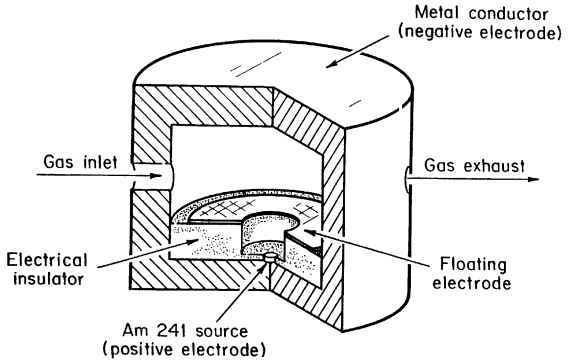

Fig. 3. Schematic of the bipolar ion chamber utilizing a floating electrode for detection and measurement of aerosols.

3. Results and analysis

3.1. DPM and combustion aerosols

Because of their simplicity, experiments could be conducted quickly resulting in a large number of experiments so that several tests under identical conditions could be used to assess the reproducibility of the data and the variations that occurred from one test to the next. In general, DPM and combustion aerosol mass concentrations varied over a broad range, from roughly zero to more than 50 or 60 mg/m^3, although in the data and analysis that follow, particular attention was paid to mass concentrations < 10 mg/m^3, since it is in this region that early warning fire detection is generally achieved. The basic data acquired are summarized as averages in the following Tables, where the averages represent measurements from typically 2–4 tests for each aerosol source. It is also worth noting that, although differences for one source, from one test to the next, did occur, these differences were generally within ± 15–20% of the average reported. Also, the sensitivities, presented in terms of the signal per unit mass concentration, were determined from linear regressions of the signals as functions of the mass concentrations. This approach is preferable to simple signals divided by the mass concentrations, because it better reflects the changes in signal per unit change in mass concentrations.

Data for the ion chamber and the dual angle light scattering module are shown in Table 1. Inspection of the data in Table 1 indicates that the ion chamber, CEV/M, is most sensitive to DPM, less sensitive to aerosols from flaming combustion, and even less sensitive to aerosols from smoldering combustion. For the angular intensity sensitivities, $\Delta I(15)/M$ and $\Delta I(30)/M$, just the reverse is true. These data confirm the hypothesis previously discussed relevant to the detector sensitivities to different types of aerosols. These results indicate that the ratios of change in ion chamber CEV to change in angular intensities, $\Delta CEV/\Delta I(15)$, $\Delta CEV/\Delta I(30)$, $\Delta CEV/(\Delta I(15)-\Delta I \times$

Table 1
Measured sensitivities, V/(mg/m^3), for diesel exhaust particles and various combustion aerosols using the bipolar ion chamber with floating collection electrode and the dual angle scattering module

Aerosol source	$\Delta CEV/M$	$\Delta I(15)/M$	$\Delta I(30)/M$	$\Delta I(15)/M-\Delta I(30)/M$
Diesel exhaust	0.2083	0.0122	0.007	0.0052
Flaming				
No. 2 Diesel fuel	0.0529	0.0884	0.0372	0.0512
Pgh seam coal	0.0457	0.0733	0.0360	0.0373
SBR	0.0684	0.0977	0.0399	0.0578
Douglas fir	0.1082	0.0755	0.0403	0.0352
Bond paper	0.1255	0.0659	0.0263	0.0396
Smoldering				
Pgh Seam coal	0.0280	0.1450	0.0760	0.0690
SBR	0.0252	0.2140	0.0888	0.1252
Douglas fir	0.0212	0.1645	0.0722	0.0923

(30)), or even the intensity difference $\Delta I(15)-\Delta I(30)$ may be sufficient to discriminate between particles produced from fires and particles produced from diesel exhausts. To determine which of these possibilities present the best discrimination capabilities, the values from Table 1 were computed as averages for the three generic sources, diesel exhaust, flaming combustion, and smoldering combustion and are shown in Table 2.

The values shown in Table 2 indicate that the ratio of ion chamber sensitivity to angular intensity difference, $\Delta CEV/(\Delta I(15)-\Delta I(30))$, provides for the greatest discrimination between fire combustion aerosols and DPM, although the ratio, $\Delta CEV/\Delta I(15)$, is comparable. For these two ratios, more than two orders of magnitude separate DPM and aerosols from smoldering fires. More than an order of magnitude separates DPM from aerosols from flaming fires, and even for fire-generated aerosols, the ratios for smoldering are a factor of 7 lower than the ratios for flaming, indicating that there exists a distinct possibility that, not only can DPM be discriminated from fire-produced aerosols, but also, that the stage of combustion may also be determined. From a practical viewpoint, the simple ratios, $\Delta CEV/\Delta I(15)$ or $\Delta CEV/\Delta I(30)$, are simpler to implement and may be more reliable than the ratio, $\Delta CEV/(\Delta I(15-\Delta I(30))$, since the latter ratio would require 3 measurements rather than 2 and additional electronics would be needed to subtract the intensities before determining the ratio. Alternatively, the intensity difference, $\Delta I \times (15)-\Delta I(30)$, also requiring only two measurements, could possibly be used. In this case, there would also be no need for the ion chamber, resulting in a simpler device, but for this alternative, the condition(s) for alarm become dependent upon the aerosol mass concentrations and no true ability to discriminate exists. The ratios, however, are independent of aerosol mass concentration, and as long as the signals are measurable with reasonable signal-to-noise ratios, high discrimination capabilities do exist.

To better understand how these ratios and discrimination capabilities would work in actual practice, it is instructive to look at the optical densities and specific extinction coefficients measured during these experiments. The optical density, D, expressed in inverse meters (m^{-1}) measured at an average wavelength of 546 nm, as previously discussed, is calculated from the transmission, T, of light through the system of aerosol particles via the expression

$$D = (1/L)\log(1/T), \tag{2}$$

where the path length, L, is constant at 1.483 m. The optical density per unit mass

Table 2
Sensitivity ratios and angular intensity differences for the three types of aerosols

Aerosol source	$\Delta CEV/\Delta I(15)$	$\Delta CEV/\Delta I(30)$	$\Delta CEV/(\Delta I(15)-\Delta I(30))$	$\Delta I(15)/M-\Delta I(30)/M$
Diesel exhaust	17.1	29.8	42.5	0.0052
Flaming combustion	1.05	2.37	1.94	0.0442
Smolder combustion	0.147	0.315	0.279	0.0955

concentration is related to the specific extinction, Q_{EXT}, in units of m^2/g, by the simple expression

$$Q_{EXT} = 2303 \cdot D/M \tag{3}$$

with the mass concentration, M, in mg/m^3. The optical density is important because Federal Regulations [16] require that when smoke detectors are used for early warning fire detection in underground coal mines, they shall provide alarm at optical densities less than $0.022\,m^{-1}$. In addition, for a detector to function reliably, the signals from both the ion chamber and the scattering module must be significantly greater than their respective noise levels. For the ion chamber CEV, the noise level, expressed as the standard deviation in the steady-state signal was determined to be ± 0.0157 V. For the $I(15)$ and $I(30)$ signals, the noise levels (standard deviations) were similarly determined and found to have values of ± 0.0115 and ± 0.005 V, respectively. To increase the reliability of the detection process, it is assumed that both the CEV and $I(15)$ voltage signals must increase by a voltage equal to 10 times their respective standard deviations. For the CEV, $I(15)$, and $I(30)$ voltages, the respective increases are 0.157, 0.115, and 0.050 V. The data for optical density are shown in column 2 of Table 3, column 3 is the mass concentration at which $D = 0.022\,m^{-1}$, column 4 is the mass concentration at which the CEV voltage increase equals 10 standard deviations (calculated using the data of column 2 of Table 1), and column 5 is the mass concentration at which the $I(15)$ voltage increase equals 10 standard deviations (calculated using the data of column 3 of Table 1).

If it is assumed that both signals must satisfy the condition of increase equal to 10 standard deviations, then from Table 3, two points are worth noting. First, the mass concentrations in columns 4 and 5 are always less than the values in column 3, meaning that reliable signals occur before the specified alarm value of optical density is reached. Second, for combustion aerosols, with the exception of flaming Douglas

Table 3
Measurements of optical density per unit mass concentration for diesel exhaust particles and combustion aerosols, along with the expected mass concentration at $D = 0.022\,m^{-1}$, the mass concentrations at an increase of 10 standard deviations of the ion chamber CEV, and the mass concentrations at an increase of 10 standard deviations of the 15° intensity

Aerosol source	D/M	M @ $D = 0.022\,m^{-1}$	M @ 10 $CEVSDs$	M @ 10$I(15)SDs$
Diesel exhaust	0.00147	15.0	0.755	9.43
Flaming				
No. 2 diesel fuel	0.00417	5.3	2.97	1.30
Pgh seam coal	0.00347	6.3	3.44	1.57
SBR	0.00395	5.6	2.30	1.18
Douglas fir	0.00327	6.7	1.45	1.52
Bond paper	0.00195	11.3	1.25	1.75
Smoldering				
Pgh seam coal	0.00315	7.0	5.61	0.79
SBR	0.00253	8.7	6.24	0.54
douglas fir	0.00205	10.7	7.42	0.70

fir and flaming bond paper, the mass concentrations at 10 standard deviation increases are greater for the ion chamber than for the light scattering module, and even for these two exceptions, the difference between the two is small.

Finally, if these voltage increases are satisfied as the initial step of the detection process, the second and final step leading to alarm is to form the ratio, $\Delta CEV/\Delta I \times (15)$, and if this ratio is less than some pre-set value, then the detector will issue an alarm. From column 2 of Table 3, the average ratio is in the range of 1.05 for FCA, although, for flaming bond paper, the calculated ratio is 1.904, and for flaming Douglas fir, the calculated ratio is 1.433. It follows from these values, that a reasonable ratio for discrimination may be in the range of 2.0. This ratio would be approximately 9 times lower than the ratio for DPM, indicating good to excellent discrimination capabilities. It should be noted, and stressed, that in mines that do not use diesel equipment, either the ion chamber or the light scattering module could stand alone, but, considering the values in columns 4 and 5 of Table 3, the light scattering module sensitivity is generally equivalent to or better than the ion chamber sensitivity to FCA, while for SCA, the light scattering module sensitivity is greater by a factor of 10. It should be noted that combustion aerosol mass concentrations calculated at increases in $I(30)$ equal to 10 standard deviations, or 0.050 V, are essentially identical to those in column 5 of Table 3. In addition, the average ratios, $\Delta CEV/\Delta I(30)$, for combustion aerosols relative to DPM, are in about the same proportions as the $\Delta CEV/\Delta I(15)$ ratios relative to DPM. This would mean that either 15° or 30°, and most probably any scattering angle lying between these two, could be used with equivalent effectiveness.

3.2. Mixtures of DPM and combustion aerosols

The data just presented were for experiments that contained only one aerosol component. Just as there is concern about measurements in DPM/dust mixtures, the typical use of the envisaged smoke detector would be one in which the sensor is continuously exposed to some level of DPM contamination and the aerosols produced from a fire would have to be detected in the presence of this contamination as the combustion aerosols mix with DPM in the mine atmosphere. To examine this scenario, tests were conducted during which DPM was flowed into the smoke box at a fixed rate resulting in a steady-state or near steady-state concentration of DPM and the establishment of constant signals from the ion chamber and the scattering module. Combustion aerosols, both from flaming combustion (a small pool flame of No. 2 diesel fuel) and smoldering combustion (from Pgh seam coal) were then diverted into the smoke box simultaneously with the DPM and the resultant changes in aerosol mass concentration, CEV, $I(15)$, $I(30)$, and optical density measured.

Now, in keeping with the prior description of the operation of the detector, four conditions must be satisfied before the detector will issue an alarm.

1. The change in CEV from its base value @ zero aerosol concentration must be greater than 10 standard deviations, or 0.157 V;

2. The change in $I(15)$ from its base value @ zero aerosol concentration must be greater than 10 standard deviations, or 0.115 V;
3. The ratio, $\Delta CEV/\Delta I(15)$, for these two signals must be <2.0; and
4. The aerosol optical density should be less than $0.022\,m^{-1}$.

The data from three tests are shown in Figs. 4–6. Fig. 4 is for a test for a FCA where the pre-existing level of DPM was $2.5\,mg/m^3$ with an optical density of $0.0037\,m^{-1}$; Fig. 5 for a SCA where the pre-existing level of DPM was $2.8\,mg/m^3$ with an optical density of $0.0041\,m^{-1}$; and Fig. 6 for a SCA where the pre-existing level of DPM was $7.55\,mg/m^3$ with an optical density of $0.0094\,m^{-1}$. In general, all three experiments show the same trends. As the combustion aerosol begins to enter the smoke chamber, all three signals begin to increase, with the $I(15)$ and $I(30)$ signals increasing more rapidly than the *CEV*. For all tests, the *CEV* from DPM is sufficient to satisfy condition 1 above. For the FCA test (Fig. 4), condition 2 is satisfied 24 s after this aerosol begins to enter the smoke chamber; condition 3 is satisfied at 36 s where the optical density is 0.020, satisfying condition 4. For the first SCA test, condition 2 is satisfied 34 s after the aerosol initially enters the smoke chamber and condition 3 is satisfied at 56 s at an optical density of $0.0135\,m^{-1}$, satisfying condition 4. For the second SCA test, condition 2 is satisfied 32 s after the aerosol initially enters the smoke chamber and condition 3 is satisfied at 54 s at an optical density of $0.020\,m^{-1}$.

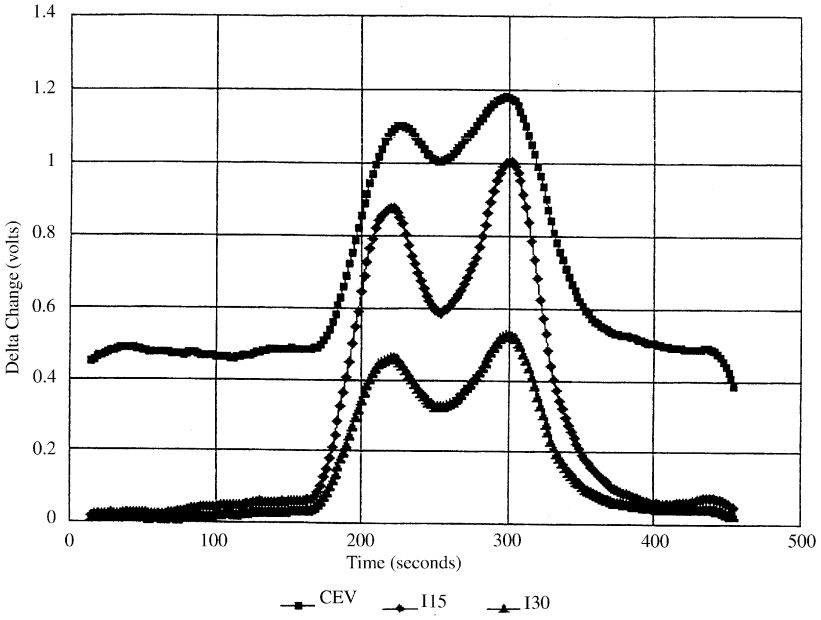

Fig. 4. Responses of the bipolar ion chamber and the scattering module to FCA generated in the presence of a pre-existing background of DPM, where the background concentration of DPM is $2.5\,mg/m^3$.

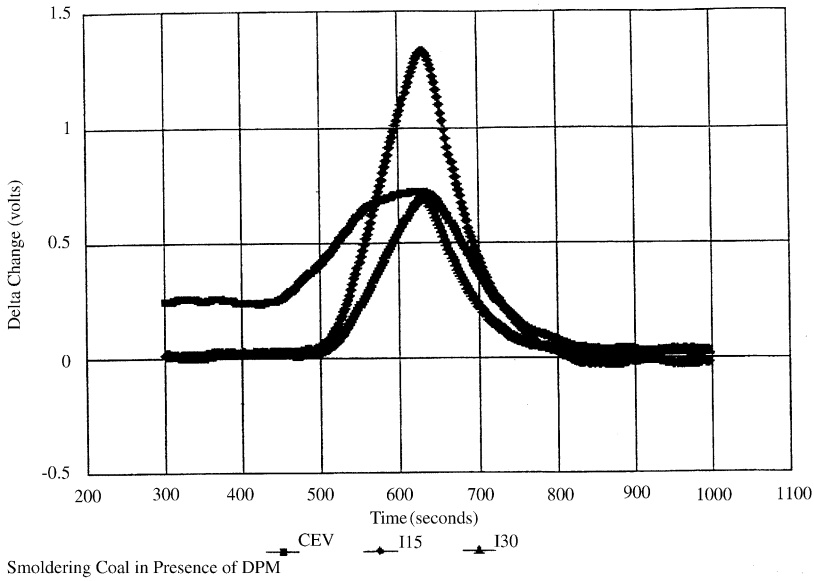

Fig. 5. Responses of the bipolar ion chamber and the scattering module to SCA generated in the presence of a pre-existing background of DPM where the background cncentration of DPM is 2.8 mg/m^3.

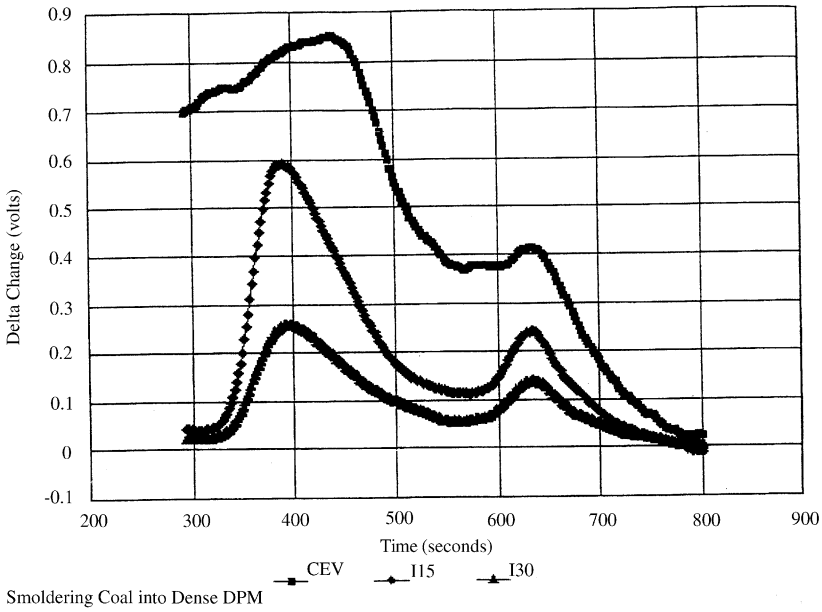

Fig. 6. Responses of the bipolar ion chamber and the scattering module to SCA generated in the presence of a pre-existing background of DPM where the background concentration of DPM is 7.55 mg/m^3.

For all three experiments, the ratio, $\Delta CEV/\Delta I(15)$, in the presence of DPM only, was in the range of 15–20. In the flaming combustion test, the ratio reached a minimum of 1.17 at a total aerosol concentration of 10.7 mg/m^3; in the first smoldering combustion test, the minimum ratio of 0.544 occurred at a total aerosol concentration of 11.3 mg/m^3; and for the second smoldering combustion test, the minimum ratio of 1.379 was reached at a total aerosol concentration of 11.2 mg/m^3 even though roughly 67% of the total mass was due to DPM. These results are extremely encouraging.

4. Conclusions

The major results of these studies, minus the analyses and embellishments, are summarized in Figs. 7 and 8, where, in Fig. 7, the sensitivities per unit mass for both the ion chamber and the second light scattering module are plotted as a function of the type of particle. The results are clear and dramatic–the ion chamber sensitivity decreases with the type of particle while the light scattering sensitivity increases. These two opposite responses, one decreasing the other two increasing, result in the ratios, $\Delta CEV/\Delta I(15)$ and $\Delta CEV/\Delta I(30)$, shown in Fig. 8, that vary by more than 2 orders of magnitude from DPM to SCA. Also shown in these figures are the measured angular intensity sensitivities for respirable coal dust, a contaminant that

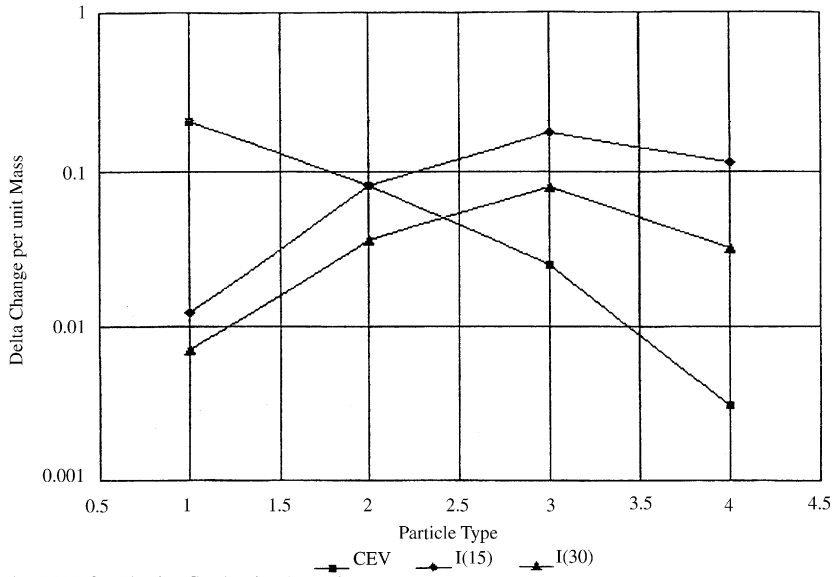

Fig. 7. The average sensitivities of the bipolar ion chamber and the scattering module for the different types of particles studied in this research.

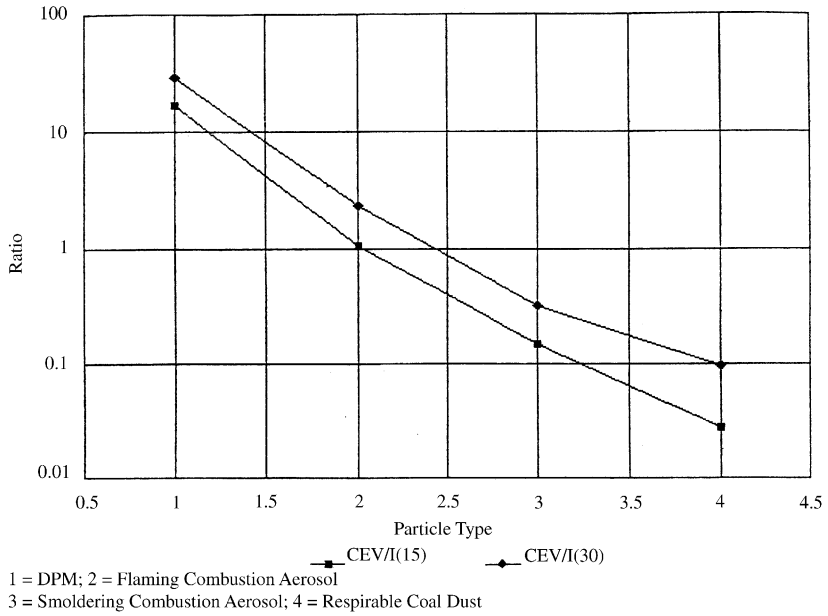

Fig. 8. The average ratios, $\Delta CEV/\Delta I(15)$ and $\Delta CEV/\Delta I(30)$, for the different types of particles studied in this research.

may also affect the reliable operation of fire detectors. For coal dust, no change in *CEV* occurred at concentrations up to about 15 mg/m^3, so to provide some measure of the *CEV* sensitivity, the measured noise level was divided by an average coal dust concentration equal to 5.0 mg/m^3.

The combination of ion chamber and light scattering module was shown to provide excellent discrimination capabilities as a fire sensor for the detection of developing fires in atmospheres contaminated by DPM, both in underground mines or in any other application where similar problems exist. The use of an alarm based upon satisfying 3 conditions for the sensor signals (the 4th condition is imposed externally) was shown to have merit in situations that are typical of normal usage. For applications where DPM contamination may not be a problem, either component could be used independently, although the light scattering approach appears to offer greater sensitivity to both types of combustion aerosols. Even in applications where DPM contamination is not a problem, the use of a combined sensor allows for the determination of the stage of the combustion process, should the need to make this determination exist. While there may be other approaches to solving this problem, the simplicity, low-cost, high sensitivity, and high discrimination capabilities of this technique offer distinct advantages. When one can purchase an ion chamber, two photodiodes, a diode laser, and some electronics for less than $80, the investigation of alternative techniques rapidly becomes a moot point.

Prototypes of these fire sensors will be fabricated for subsequent test and evaluation in underground mines and in other applications where similar needs exist.

References

[1] Smith CL. Smoke detector operability survey. Report on Findings. US Consumer Product Safety Commission, October 1994. 98pp.
[2] Smith LE. Fire incident study. National Smoke Detector Project. US Consumer Product Safety Commission, January 1995. 61pp.
[3] Grosshandler WL editor. Nuisance alarms in aircarft cargo areas and critical telecommunications systems. Proceedings of the Third NIST Fire Detector Workshop, NISTIR 6146, BFRL, NIST, March 1998. 34pp.
[4] Mulholland GW, Croarkin C. Specific extinction coefficient of flame generated smoke. Fire Mater 2000;24(5):227–30.
[5] Choi MY, Mulholland GW, Hamins A, Kashiwagi T. Experimental study of the optical properties of soot and smoke. NISTIT 5499, NIST, Annual Conference on Fire Research: Book of Abstracts, October 1994. p. 123–4.
[6] Sorensen CM, Feke GD. Post-flame soot. Proceedings of the International Conference on Fire Research and Engineering (ICFRE), September 1995. p. 281–5.
[7] Mulholland GW, Johnsson EL, Shear DA, Fernandez MG. Design and testing of a new smoke concentration meter. Proceedings of the Fall Conference. Fire Retardant Chemicals Association (FRCA), October 1998. p. 41–9.
[8] Gottuk DT, Peatross MJ, Roby RJ, Beyler CL. Advanced fire detection using multi-signature alarm algorithms. Proceedings of the International Conference on Automatic Fire Detection AUBE 99, March 1999. p. 237–46.
[9] Milke JA. Application of neural networks for discriminating fire detectors. Proceedings of the International Conference on Automatic Fire Detection AUBE 95, April 1995. p. 213–22.
[10] Grosshandler WL. Review of measurements. Candidate Signatures for Early Fire Detection. NISTIR 5555, BFRL, NIST, January 1995. 36pp.
[11] Brinn M, Bott B. A fresh approach to mine fire detection. Trans Inst Min Eng 1994; 71–4.
[12] Litton CD, Conti RS, Tabacchi JG, Grace R. Evaluation of a nitric oxide-compensated carbon monoxide fire sensor. BuMines IC 9339, 1993. 10pp.
[13] Litton CD. Fractal properties of smoke produced from smoldering and flaming fires. Proc ASME Int Mech EngCongr Exposition, Dallas, TX, HTD 1997;352:119–34.
[14] Edwards JC, Morrow GS. Development of coal combustion sensitivity tests for smoke detectors. US Bureau of Mines Report of Investigations 9551, 1995. 12pp.
[15] Patashnick H, Rupprecht G. Microweighing goes on-line in real time. Res Dev 1986;28(6):74–8.
[16] Title 30, US Code of Federal Regulations, Part 75.351, July 1, 1995. p. 479.